HabEx Space Telescope Optical System Overview: General Astrophysics Instruments

Stefan Martin, Mayer Rud, Paul Scowen*, Daniel Stern, Joel Nissen
Jet Propulsion Laboratory, California Institute of Technology, Pasadena, CA 91109.
*Arizona State University, Tempe, AZ 85287.

ABSTRACT

The HabEx (Habitable Exoplanet) concept study is defining a future space telescope with the primary mission of detecting and characterizing planetary systems around nearby stars. The telescope baseline design includes a high-contrast coronagraph and a starshade to enable the direct optical detection of exoplanets as close as 70 mas to their star. In addition to the study of exoplanets, HabEx carries two dedicated instruments for general astrophysics. The first instrument is a camera enabling imaging on a 3 arc minute field of view in two bands stretching from the UV at 150 nm to the near infrared at 1800 nm. The same instrument can also be operated as a multi-object spectrograph, with resolution of 2000. The second instrument is a high-resolution UV spectrograph operating from 300 nm down to 115 nm with up to 60,0000 resolution. HabEx would provide the highest resolution UV/optical images ever obtained. Diffraction limited at 0.4 µm, it would outperform all current and approved facilities, including the 30 m class ground-based extremely large telescopes (ELTs), which will achieve ~0.01 arcsecond resolution at near-infrared (IR) wavelengths with adaptive optics, but will be seeing-limited at optical wavelengths. HabEx would observe wavelengths inaccessible from the ground, including the UV and in optical/near-IR atmospheric absorption bands. Operating at L2, far above the Earth's atmosphere and free from the large thermal swings inherent to HST's low-Earth orbit, HabEx would provide an ultra-stable platform that will enable science ranging from precision astrometry to the most sensitive weak lensing maps ever obtained. Here we discuss the design concepts of the general astrophysics optical instruments for the proposed observatory.

Keywords: HabEx, space telescope

1. INTRODUCTION

In the tradition of NASA Great Observatories such as Hubble SpaceTelescope (HST), the future James Webb Space Telescope (JWST), and Wide Field Infrared Survey Telescope (WFIRST), HabEx would have at least 25% of the primary mission and most of an extended mission reserved for guest observers. With the largest aperture ultraviolet (UV)/optical mirror ever deployed in space and two powerful instruments designed for this aspect of the mission, it would enable unique science, not possible from ground or space-based facilities even in the 2030s, when HabEx would launch. This science would be broad and exciting, addressing the full range of primary NASA science disciplines, from solar system investigations to Cosmic Origins (COR) science to Physics of the Cosmos (PCOS). Furthermore, in addition to its capability for exoplanet direct imaging, HabEx would enable additional exoplanet exploration science, including transit spectroscopy and imaging of protoplanetary disks. Guest Observer (GO) time encompasses everything beyond the planned exoplanet direct imaging survey, and these competed programs are referred to as "observatory science." It is expected that HabEx

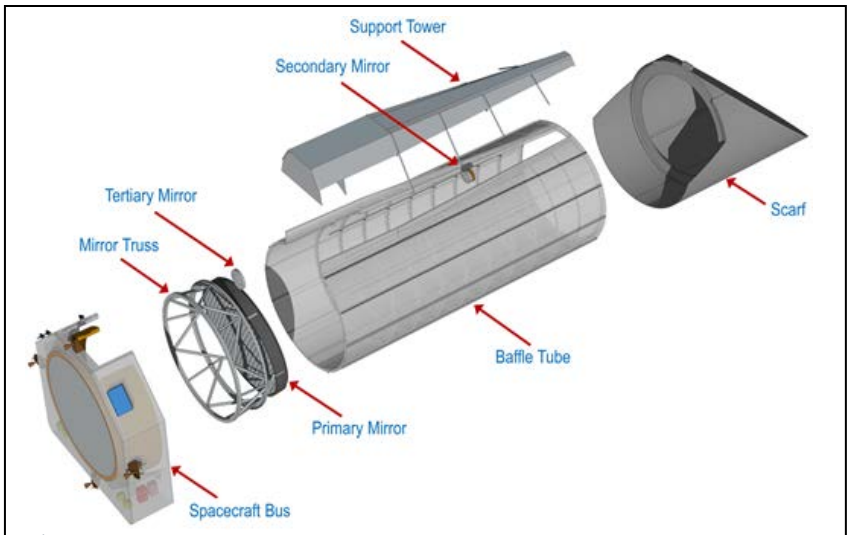

Figure 1:

would serve a very similar role to that played by HST in the astronomical community and the world at large for decades: a flexible and powerful tool producing an extremely broad range of exciting astrophysics, and fueling the public's interest in science, the cosmos, and NASA.

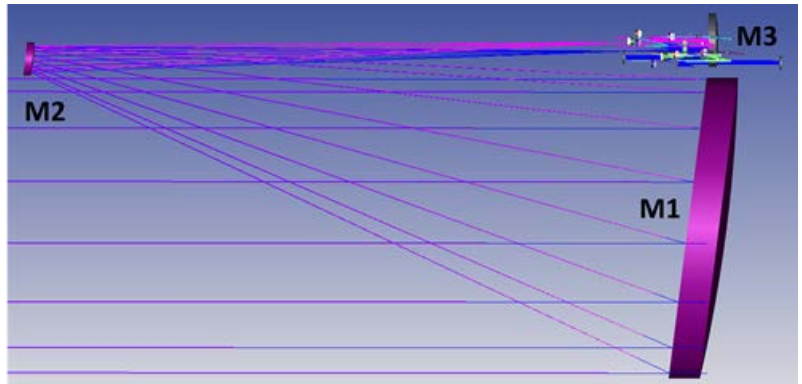

Figure 2: Telescope optical layout. The instruments are arranged near M3.

The HabEx telescope[1,2] is a three mirror anastigmat design (TMA) with a 4-m diameter primary mirror, 2.5-m off axis. A 4 m primary mirror directs light to the secondary then on to the tertiary, producing a collimated 50 mm beam at the output. Figure 1 shows the telescope's principal structural components. The instruments are arranged near the tertiary mirror, extending into the secondary support tower. The telescope structure is designed to provide the superior stability[3] necessary required for coronagraphy at 10^{-10} contrast. The primary mirror truss is connected to the secondary mirror by a rigid secondary mirror support tower. To maximize stiffness, the tower is integral with the stray light baffle tube. The tube and its internal stray light baffles provide lateral and bending stiffness support but, because the telescope is off-axis, the internal baffles are discontinuous and so corresponding external gussets complete the support.

The optical design allows for different optical coatings at different locations on the tertiary, or separate tertiary mirrors with instrument-specific coatings, to aid transmission efficiency with the various instruments. The general astrophysics (GA) instruments, a high resolution UV spectrograph (UVS)[1,4] and a general purpose camera/spectrograph, the HabEx Workhorse Camera (HWC)[1] respectively require performance down to 115 nm and 150 nm in the UV, so a protected aluminum coating is required on the mirrors in those beam trains. The four science instruments are arranged on the side of the telescope near M3 as shown in Figure 2. The two exoplanet instruments are described elsewhere[5]; in this paper we focus on the GA instruments.

The two GA instruments are included in the HabEx design specifically to enable a wide range of observatory science programs. Both instruments rely on low-risk, flight-proven technology, and neither places strong additional requirements on the observatory design. The UVS is an evolved version of HST's COS[6], taking advantage of several decades of improvement in detector and optics technology, as well as the larger aperture of HabEx. The latter is an evolved version of the dual-beam Wide-Field Camera 3 (WFC3[7]) on HST. HWC would provide imaging and multi-slit spectroscopy in two channels: a UV/optical channel, and a near-IR channel. The UVS would access the large number of diagnostic emission and absorption lines available at wavelengths shorter than 300 nm. The driving science cases include understanding the life cycle of baryonic material as it is moved in and out of galaxies and into stars and planets, determining the escape fraction of hydrogen-ionizing photons from star-forming galaxies and whether this can explain the reionization of the universe at early ages, and the life cycle and impact of massive stars on their environments and the subsequent generations of stars and planets that follow the first generation of massive stars. The needed capabilities include a wide field of view, the ability to perform multi-object spectroscopy (MOS) within that field and access to the shortest wavelengths possible while taking account of the requirements of the other instruments on the telescope. Exoplanet observations would be carried out both in tandem with and separately from GA observations. Aside from dedicated GA time, opportunistic observing is possible on both the UVS and HWC simultaneously when either the starshade or coronagraph instruments are being used. This is because each instrument has its own field of view on the sky as shown in figure 3. As a TMA, the telescope generates a well-corrected field of view with

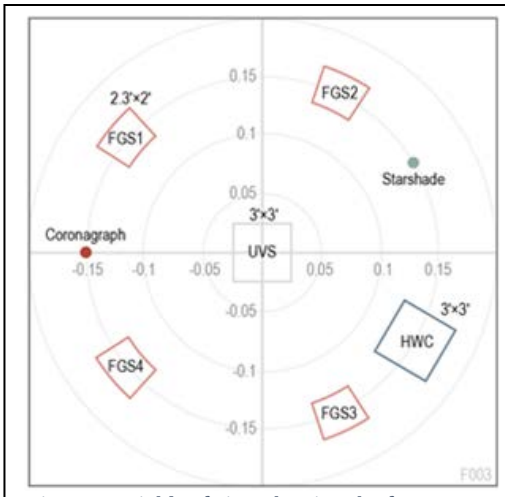

Figure 3: Fields of view showing the four science instruments and the fine guiding system areas.

an annular shape, in this case with a radius of 0.15°. As seen in the figure the starshade and coronagraph have small fields of view ~0.3° apart, while the UVS occupies a 3'x3' field on axis. The HWC occupies a separate 3'x3' field. Other portions of the telescope field are taken up by the fine guidance system (FGS). This system enables extremely good pointing control and particularly control of roll which is needed for coronagraph operations. The on-axis UVS field is also fairly well corrected, having a slowly varying wavefront error.

Parallel observations with the exoplanet direct imaging program would enable multiple ultra-deep imaging fields, similar to the extremely successful Hubble Deep Fields and Hubble Ultra-Deep Survey. In addition, ultra-deep spectroscopic surveys done in parallel with the exoplanet direct imaging observations would enable a range of science, from ultra-deep probes of the IGM with UVS, to ultra-deep and/or highly complete spectroscopic surveys with HWC. The UVS and HWC fields of view are sufficiently offset from the direct imaging instrument fields of view that scattered light is not expected to be an issue, and the HWC instrument design incorporates a fine steering mirror enabling scene dithering during the deep exoplanet stares.

2. GENERAL ASTROPHYSICS INSTRUMENTS

2.1 An Ultraviolet Spectrograph

The UVS instrument enables high-resolution spectroscopy down to 115 nm in the UV. The baseline design enables transmission down to 115 nm using Al coated mirrors protected with MgF2, and there is a stretch goal of reaching down to 100 nm using Al mirrors protected using LiF and either AlF3 or MgF2 deposited using atomic layer deposition (ALD). Such a goal depends on future developments in these mirror coatings for the UV; current mirror coatings which will transmit at shorter wavelengths unfortunately compromise performance elsewhere in HabEx's wavelength range.

The UVS utilizes a microshutter array[8] (MSA) based on the design incorporated into JWST, situated at the two-mirror Cassegrain focus to enable selection of objects of interest from a 3'×3' FOV. Table 1 shows key design parameters. A range of spectral resolutions is provided to enable measurement of both line shape and separation of specific lines in both emission and absorption. With a maximum resolution of 60,000, the UVS carries a large set of gratings to cover the wavelength bands shown in Table 2. The detector area is large, requiring about 30,000×17,000 pixels (or "pores" in the case of microchannel plate detectors) to cover the FOV. This area would be covered using a 3×5 array of approximately 100×100 mm microchannel plate (MCP) detectors, or alternatively, a larger array of delta doped UV-optimized CCDs. Both types of detector have similar performance and technology readiness levels.

Table 1: Key UV spectrograph requirements.

UV Spectrograph Requirements	
Waveband:	115–300 nm minimum
Field-of-view:	2.5×2.5 arcmin (3'x3' designed)
Spectral resolution:	R ≥ 60,000 (highest resolution bands)
Throughput:	> 10%
Pointing: • Accuracy: • Stability:	 • 2 mas rms/axis • 2 mas rms/axis

Telescope wavefront error results in the design being diffraction limited at 400 nm so that the Nyquist sampled angular resolution at the image plane is 20.6 mas. For a 3' wide FOV, the focal plane is therefore ~17,500 pixels wide. In the spectral domain, the criterion for spectral elements to be resolved is the same so that a spectral resolution element $\Delta\lambda$ covers two pixels. For example, with R = 60,000 at 120 nm, $\Delta\lambda$ = 2 pm (Table 3) and the number of spectral elements needed to cover the first band which is 12 nm wide is 6,000. Thus, a single spectrum on the detector would cover 12,000 pixels, resulting in the rectangular shape of the focal plane. Because of the relatively low reflectance of available mirror coatings in the UV (the reflectivity of aluminum is ~81% at 120 nm), it is important to minimize the number of reflections from the primary mirror to the focal plane. Therefore, a conventional multiple

Table 2: UV spectrograph design

FOV	3'×3'
Wavelength bands	20 bands covering 115 to 300 nm
Spectral resolutions	60,000 25,000 12,000 6000 3000 1000 500 1
Imaging resolution	10.3 mas per pixel
Detector	3×5 MCP array, 100 mm sq each
Array width	17,500 × 30,000 pixels (pores)
Microshutter aperture array	2×2 array of 171×365 200×100 μm apertures

mirror approach following the tertiary mirror is precluded. The optical design is constrained by the prescription of the telescope's first two mirrors and a wide design space was explored to reach the solution.

After extensive trials, a design with just four reflections was arrived at. In that design, shown in Figure 4, the beam from an off-axis tertiary mirror strikes a powered grating before falling on the focal plane. The system resides in front of the main tertiary mirror. This 4-reflection design yielded 50% throughput at 125 nm. It requires fairly large gratings, about 100 mm diameter, so the set of gratings would be mounted in two rows set into a wheel of ~0.5-m diameter.

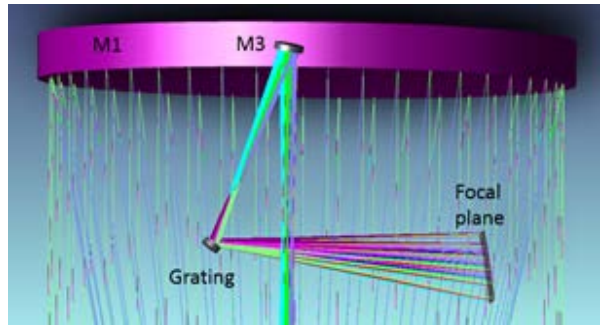

Figure 4 High-resolution UVS. Light from the telescope secondary mirror strikes a dedicated M3 and then the grating before arriving at the focal plane. The other optical systems around this area are not shown.

The best-corrected focus available is on axis at the Cassegrain focus formed by the primary and secondary mirrors, so this is where the MSA is located. The tertiary mirror is an off-axis aspheric surface modified by polynomial and Zernike terms, producing a beam focused near the detector. The grating, located a little beyond the exit pupil is weakly aspheric and carries an unevenly spaced groove pattern with approximately 2 µm spacing for the shortest wavelength and highest dispersion. This surface can be fabricated using conventional optical polishing plus electron beam lithographic techniques. The resultant design yields the 3'×3' field, corrected at the telescope diffraction limit of 400 nm. Gratings are individually optimized for each waveband and the design includes one optic without grating lines, so that an undispersed UV image is formed.

The detector is a photon-counting device consisting of a MCP array utilizing large-format plates about 100 mm wide. The MCPs are glass capillary arrays (GCAs) consisting of thin-walled hexagonal tube assemblies, and are fabricated in very low-Pb glass for a low x-ray cross section. The tubes (micropores) are arranged with a small angle typically ~15 degrees off normal. Each plate consists of a micropore array of two layers with opposing pore angles for efficiency. Furthermore, the materials used are very pure and contain few radioactive isotopes, leading to a very low dark count. Atomic layer deposition (ALD) is used to create the resistive and emissive layers (GaN and multi-alkali) of the cathode, producing improved performance specifications over conventional MCPs. The assembled plate is enclosed in a frame and covered with a MgF2 window, also coated, so that a high vacuum can be pulled to assure long-term performance of the emissive layers during I&T through to launch. One hundred mm square MgF2 windows are considered possible with the large crystal boules now being made. A 3×5 array of MCPs produces a 3'×3' field of view with the long axis accommodating the spectral dispersion. Since the plates are surrounded by the frame of the vacuum assembly there would be small gaps of coverage as is often the case with detector arrays.

Beneath each plate a lattice of wires forms the anode. Incoming UV photons produce a cascade of electrons with gain of 10^6 or more, and the charge cloud emerges at the base of the MCP assembly to impact the anode wires. High-speed analog to digital converters (ADCs) digitizing 8 bits at 10 MHz, collect charge from the wires. An ASIC postprocessor outputs a stream of data consisting of charge cloud centroid position (x and y), peak height, coincidence flag, and time stamp. In the case of two or more photons arriving at the same time, the postprocessor rejects the event based on peak height. Behind the anode is a plastic scintillator viewed by a miniature avalanche photodiode or photomultiplier tube that acts as a cosmic ray detector. In the case of a detection here coincident with an event on the wire grid, the coincidence flag is set and the event rejected. Thus, a clean signal can be generated in the presence of a cosmic ray background.

Table 3. Spectral bands for UVS instrument.

Resolution R	λ min	λ max	Δλ	Resolution R	λ min	λ max	Δλ
λ/Δλ	nm	nm	pm	λ/Δλ	nm	nm	pm
60,000	115	127	2.01	25,000	115	146	5.41
60,000	127	139	2.21	25,000	146	186	6.88
60,000	139	153	2.44	25,000	186	236	8.74
60,000	153	169	2.68	25,000	236	300	11.11
60,000	169	186	2.95	12,000	115	186	12.29
60,000	186	204	3.25	12,000	186	300	19.86
60,000	204	225	3.58	6,000	115	300	32.15
60,000	225	248	3.94	3,000	120	300	64.29
60,000	248	273	4.33	1,000	120	300	185.00
60,000	273	300	4.77	500	120	300	185.00

The spatial digitization is at the micropore spacing. While the charge cloud spreads upon emission from the base of the plates, the large electron count allows localization of the event at the micropore level. The ADC rate (10 MHz), a determinant of photon flux, can handle up to ~10^7 photons/sec with an efficiency loss due to the coincidence of a portion of events. The majority of science targets will be much weaker, so that typically hundreds of objects may be observed simultaneously.

2.2 A Workhorse Camera

The HabEx workhorse camera is a general purpose instrument providing UV through near-IR imaging and multi-object spectroscopy, with objectives ranging from solar system science to detailed studies of galaxies and quasars at the epoch of reionization to cosmology. The HWC would enable detailed follow-up of interesting targets, such as those identified from the wide-field surveys of the 2020s, such as Euclid, LSST, and WFIRST. Specifically, the instrument is designed to provide unique scientific capabilities compared to the facilities expected in the 2030s. For example, nearly all of the first-generation instruments on the new 30 m class telescopes (e.g., TMT, GMT, and ELT) are near-IR instruments because ground-based adaptive optics (AO) is not expected to be effective for wavelengths much shorter than about 1 µm. The HWC would provide both unique capabilities, including: (1) UV science, (2) high spatial resolution imaging, (3) a stable platform for both photometry and morphology, and (4) access to spectral regions inaccessible on the ground due to telluric absorption.

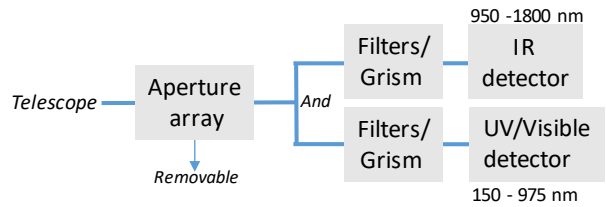

Figure 5: Workhorse camera and spectrograph schematic.

The design, like the Wide-Field Camera 3 (WFC3) on the HST, has two channels that can simultaneously observe the same field of view. An optical channel using delta-doped CCD detectors provides good throughput from 150 nm to 950 nm, and a near-IR channel using Hawaii-4RG HgCdTe arrays provides good throughput from 950 nm to 1.8 µm, at which point thermal backgrounds dominate over most celestial targets.

Table 4: HWC design specifications.

	UV/VIS Channel	IR Channel
FOV	3'×3'	3'×3'
Wavelength bands	150–400 nm 400–950 nm	950–1,800 nm Stretch goal >=2.5 µm
Pixel resolution	15.5 mas	24.5 mas
Telescope resolution	30.9 mas	49 mas
Design wavelength	600 nm	950 nm
Detector	3×3 CCD203	2×2 H4RG10
Detector array width	12,288 pixels	8,192 pixels
Spectrometer	R = 2,000	R = 2,000
Microshutter array	2×2 arrays; each array 200×100 µm aperture size with 171×365 apertures	

Both channels would have imaging and spectroscopic modes, and a MSA assembly provides for slit spectroscopy of targeted sources, significantly reducing the backgrounds and source confusion compared to the slit-less spectroscopic modes available on HST. The two modes of operation share the same optical path and cameras as shown schematically in figure 5. In the spectrographic mode, the MSA and grism sets are introduced into the beam paths. It is intended that the MSA be attached to a mechanism and thereby removable for best imaging function. Table 4 shows the design parameters for the two channels. For good imaging, the pixel spacing is chosen to Nyquist sample the PSF. To obtain sufficient field of view, the visible channel has a 3×3 array of 4k square CCD detectors, and the IR channel utilizes 2×2 H4RG10.

Figure 6 shows the optical ray traces and preliminary mechanical layout of the instrument. After reflecting off M3 and the fold mirror, the input beam strikes a fine steering mirror used for image dithering and small pointing adjustments and is normally fixed during an observation. The beam then passes through a relay formed by a pair of biconic paraboloidal mirrors, then on to a dichroic where the UV/visible light is separated from the IR light. Note that this system, while efficient in terms of throughput, does limit optical performance at the shorter wavelengths. Improved imaging below 600 nm would be achieved using additional optics to form the relay, at the expense of throughput in the UV. This is one area for a trade study. In spectroscopy mode, a microshutter aperture array is inserted into the focal plane of the relay, enabling selection of particular targets. This array is identical to the set of arrays installed in JWST Near-Infrared Spectrograph (NIRSPEC[9]) (STScI).

UV/Visible Channel

At the dichroic, UV and visible light is reflected and passes through a filter wheel to a camera. The filter wheel is mounted at a pupil plane and enables selection of different wavelengths of interest in the image with capability similar to WFP3. A grism is also placed in the wheel to allow spectroscopy in conjunction with the MSA at R = 2000. The camera consists of a three-mirror relay and the focal plane itself. Performance is diffraction limited at 600 nm. The focal plane is designed for Nyquist sampling of the 3'×3' field at the same wavelength. The selected array is CCD203, a conventional low noise CCD with 12 µm pixel size and 4k×4k format. A set of nine of these CCDs, cooled to 153K, forms the focal plane. For UV performance these arrays would be deep depletion, delta doped devices[10].

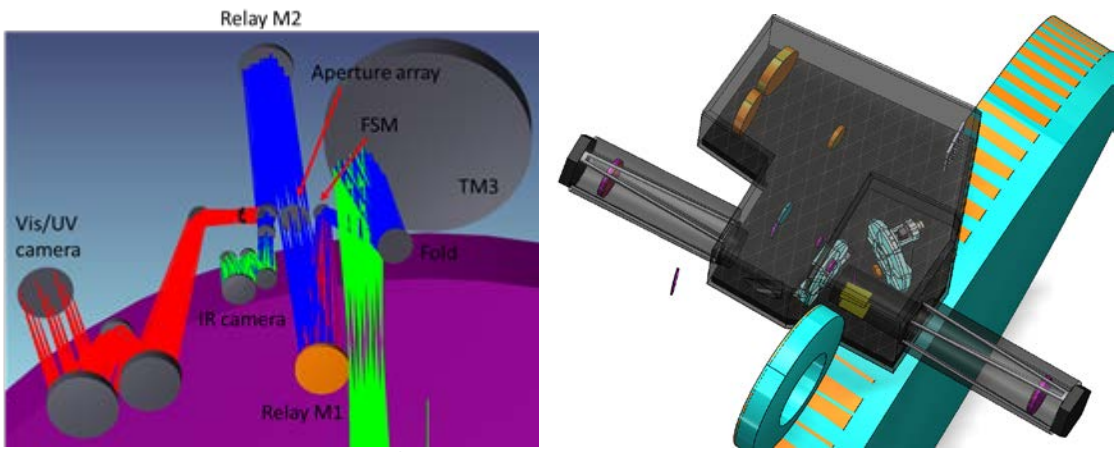

Figure 6: HabEx Workhorse Camera: left, optical components and ray traces. Right: mechanical envelope near M1.

Infrared Channel

At the dichroic, infrared light 950 to 1,800 nm is transmitted and passes through a filter wheel to a camera. As in the UV/visible channel, the filter wheel is mounted at a pupil plane and enables selection of different wavelengths of interest in the image. Again, a grism is placed in the wheel to allow spectroscopy in conjunction with the MSA at R = 2,000. The camera consists of a three mirror relay leading to the focal plane. Performance is diffraction limited at 950 nm. The focal plane is designed for Nyquist sampling of the 3'×3' field at the same wavelength. The selected array is the Teledyne H4RG10, a low noise hybrid HgCdTe/CMOS bump-bonded array with 10 um pixel size and 4k×4k format. These focal plane arrays (FPAs) are currently being developed for WFIRST. A set of four FPAs cooled to 100K forms the focal plane.

Filters

The Hubble Space Telescope's Wide Field Camera 3 carries a large set of filters with 48 slots in the UV/visible channel and 18 slots in the IR, including grisms. Some of the visible slots carry 'quad filters' so the total filter complement is larger, but these filter sets form the basis for the filters on HWC. On WFC3, the larger set was accommodated in a device known as SOFA[12] consisting of 12 wheels each carrying four slots plus one open position and a similar format will be required to fit into HWC. On the IR side, an 18 slot wheel has a large radius, so this will likely be broken up into at least two wheels as the design evolves.

3. SUMMARY

The three key capabilities demanded by HabEx's general astrophysics science programs are:

1. High-resolution ($R \leq 60{,}000$), multi-object UV slit spectroscopy to ≤ 0.115 μm;

2. Imaging and multi-object slit spectroscopy from the near-UV to the near-IR over a field of view of at least 2.5 arcmin on a side; and

3. Ability to track solar system objects.

The two HabEx GA instruments in conjunction with the excellent pointing control offered by the spacecraft bus are able to provide all these capabilities. The baseline HabEx 4 m observatory is capable of collecting three times as many photons as the 2.4 m Hubble Space Telescope. Its diffraction resolution limit is 21 milliarcseconds at 400 nm, compared to HST's performance of 34.4 mas. HabEx is designed to be the most stable astronomical observing platform ever; capable of relative pointing stability to 0.7 mas. HST's best pointing stability is ~2 mas. To ensure LOS pointing and wavefront stability at the levels required for high contrast coronagraphy, the telescope includes precision thermal control, mirror positional control using laser metrology and a fine-guiding sensor (FGS) paired with microthrusters for pointing control during observations. Furthermore, this design concept is based solely on manufacturing capabilities and state of the art telescope technologies presently available.

It is difficult to predict future science needs but by providing an excellent general purpose capability on HabEx a wide range of intriguing science programs would come within reach. Such programs include: 1) Tracing the life cycle of baryons; one third of baryons in the universe remain unaccounted for, 2) Measurements of the local value of the Hubble Constant have been controversial, and hint at possible new physics. One set of observations is based on an extensive Hubble program using WFC3 of imaging nearby galaxies at optical and near-IR wavelengths[12]. This study finds a local value of the Hubble constant that is 3.4σ higher than the latest value measured by the Planck satellite, 3) Measuring the star formation histories of nearby galaxies from stellar archaeology, 4) Probing the nature of dark matter with dwarf galaxies, 5) Exoplanet transit spectroscopy, 6) Solar system observations.

ACKNOWLEDGEMENTS

The information in this paper is provided prior to any decisions or commitments being made and is provided for planning and discussion purposes only. This work was conducted at the Jet Propulsion Laboratory, California Institute of Technology, under contract with the National Aeronautics and Space Administration. Copyright 2018 California Institute of Technology. Government sponsorship acknowledged. All rights reserved.

REFERENCES

[1] Stefan Martin, Mayer Rud, Paul Scowen, Daniel Stern, Joel Nissen, John Krist, "HabEx space telescope optical system", Proc. SPIE. 10398, 5 September 2017

[2] H. Philip Stahl, "Habitable exoplanet imager optical telescope concept design", Proc. SPIE. 10398, 5 September 2017.

[3] J. Brent Knight, H. Philip Stahl, Andy Singleton, Ron Hunt, Melissa Therrell, Kate Caldwell, Jay Garcia, Mike Baysinger, "Dynamic/jitter assessment of multiple potential HabEx structural designs", Proc. SPIE. 10374, 6 September 2017.

[4] Paul Scowen, Daniel Stern, Rachel Somerville, Mayer Rud, Stefan Martin, Matthew Beasley, "Science and architecture drivers for the HabEx Ultraviolet Spectrograph (UVS)", Proc. SPIE. 10398, 5 September 2017.

[5] Stefan Martin, Mayer Rud, Dimitri Mawet, Joel Nissen, Stuart Shaklan, Luis Marchen, "HabEx Space Telescope Exoplanet Instruments" Proc. SPIE 10698, 2018.

[6] James Green, Erik Wilkinson, Jon Morse, "The Cosmic Origins Spectrograph", Proc. SPIE. 4854, 24 February 2003

[7] John MacKenty, Sylvia Baggett, Gabriel Brammer, Bryan Hilbert, Knox Long, Peter McCullough, Adam Riess, "HST/WFC3: new capabilities, improved IR detector calibrations, and long-term performance stability", Proc SPIE 9143, 28 August 2014.

[8] Mary Li, Tomoko Adachi, Christine Allen, Sachi Babu, Sateesh Bajikar, Michael Beamesderfer, Ruth Bradley, Kevin Denis, Nick Costen, Audrey Ewin, David Franz, Larry Hess, Ron Hu, Kamili Jackson, Murzy Jhabvala, Dan Kelly, Todd King, Gunther Kletetschka, Alexander Kutyrev, Barney Lynch, Timothy Miller, Harvey Moseley, Vilem Mikula, Brent Mott, Lance Oh, James Pontius, David Rapchun, Chris Ray, Eric Schulte, Scott Schwinger, Peter Shu, Robert Silverberg, Wayne Smith, Steve Snodgrass, David Sohl, Leroy Sparr, Rosalind Steptoe-Jackson, Valeriano Veronica, Liqin Wang, Yun Zheng, Chris Zincke, "MEMS microshutter arrays for James Webb Space Telescope", Proc. SPIE. 6415, 20 December 2006

[9] Maurice te Plate, Wolfgang Holota, Winfried Posselt, Jess Koehler, Markus Melf, Giorgio Bagnasco, Pierangelo Marenaci, Opto-mechanical design of the near-infrared spectrograph NIRSpec, Proc. SPIE. 5904, 18 August 2005

[10] Nikzad, Shouleh, Michael E Hoenk, Frank Greer, Blake Jacquot, Steve Monacos, Todd J Jones, Jordana Blacksberg, Erika Hamden, David Schiminovich, and Chris Martin. "Delta-doped electron-multiplied CCD with absolute quantum efficiency over 50% in the near to far ultraviolet range for single photon counting applications." Applied Optics 51 (3):365-369, 2012.

[11] http://www.moog.com/products/actuators-servoactuators/space/spacecraft/optical-filter-wheel-assemblies.html

[12] Riess, Adam G, Lucas M Macri, Samantha L Hoffmann, Dan Scolnic, Stefano Casertano, Alexei V Filippenko, Brad E Tucker, Mark J Reid, David O Jones, and Jeffrey M Silverman. 2016. "A 2.4% Determination of the Local Value Of The Hubble ConstanTBased on observations with the NASA/ESA Hubble Space Telescope, obtained at the Space Telescope Science Institute, which is operated by AURA, Inc., under NASA contract NAS 5-26555." The Astrophysical Journal 826 (1):56.